Check for updates

Foldameric receptors with domain-swapping cavities capable of selectively binding and transporting monosaccharides†

Geunmoo Song, Seungwon Lee and Kyu-Sung Jeong [ID] *

The development of synthetic receptors capable of selectively binding and transporting saccharides is crucial but highly challenging. In this study, two foldameric receptors **1** and **2**, consisting of two repeating monomers, indolocarbazole and naphthyridine units, with different aromatic spacers in the middle of their sequences, have been synthesised. These receptors fold into helical conformations, and the two strands of each receptor are assembled to create domain-swapping cavities for binding monosaccharides by multiple hydrogen bonds. According to ^{1}H NMR, CD spectroscopy, mass spectrometry, and ITC experiments, receptor **1** forms two distinct 2 : 2 complexes with methyl β-D-galactopyranoside and methyl β-D-glucopyranoside: (**1**-*MM*)$_2$ ⊃ (methyl β-D-galactopyranoside·2H$_2$O)$_2$ and (**1**-*MP*)$_2$ ⊃ (methyl β-D-glucopyranoside)$_2$. Despite being composed of identical foldamer strands, these two complexes exhibit notably different folding and assembly modes to achieve optimal stability. The binding affinities of **1** for methyl β-D-galactopyranoside and methyl β-D-glucopyranoside are estimated to be log K = 12.7 and 13.3, respectively, in 5% (v/v) DMSO/CH$_2$Cl$_2$. On the other hand, receptor **2** forms a stable 2 : 2 receptor/guest complex with methyl β-D-glucopyranoside, (**2**-*MP*)$_2$ ⊃ (methyl β-D-glucopyranoside)$_2$, with an association constant of log K = 13.9, which is significantly higher than that of methyl β-D-galactopyranoside (log K = 11.1) and methyl α-D-glucopyranoside (log K = 10.6). Furthermore, receptor **2** facilitates the selective transport of methyl β-D-glucopyranoside over other glycosides across an organic phase (CH$_2$Cl$_2$) in U-tube experiments.

Introduction

Saccharides play crucial roles in various biological processes, including cell recognition, signaling, and immune responses.[1] Over the past several decades, significant efforts have been dedicated to the development of synthetic receptors capable of selectively binding saccharides in supramolecular chemistry.[2,3] However, the rational design of such synthetic receptors remains highly challenging owing to the structural and functional group similarities among saccharides.[4] In addition, multiple equilibria between constitutional isomers (*e.g.*, furanose *vs.* pyranose, α *vs.* β, and cyclic *vs.* acyclic forms) of simple monosaccharides provide further difficulties in the design of synthetic receptors.

Recently, we described a novel approach for developing synthetic receptors capable of selectively binding monosaccharides utilising two key principles: dynamic covalent chemistry and complexation-induced equilibrium shift.[5,6] This method

Department of Chemistry, Yonsei University, Seoul 03722, South Korea.
E-mail: ksjeong@yonsei.ac.kr

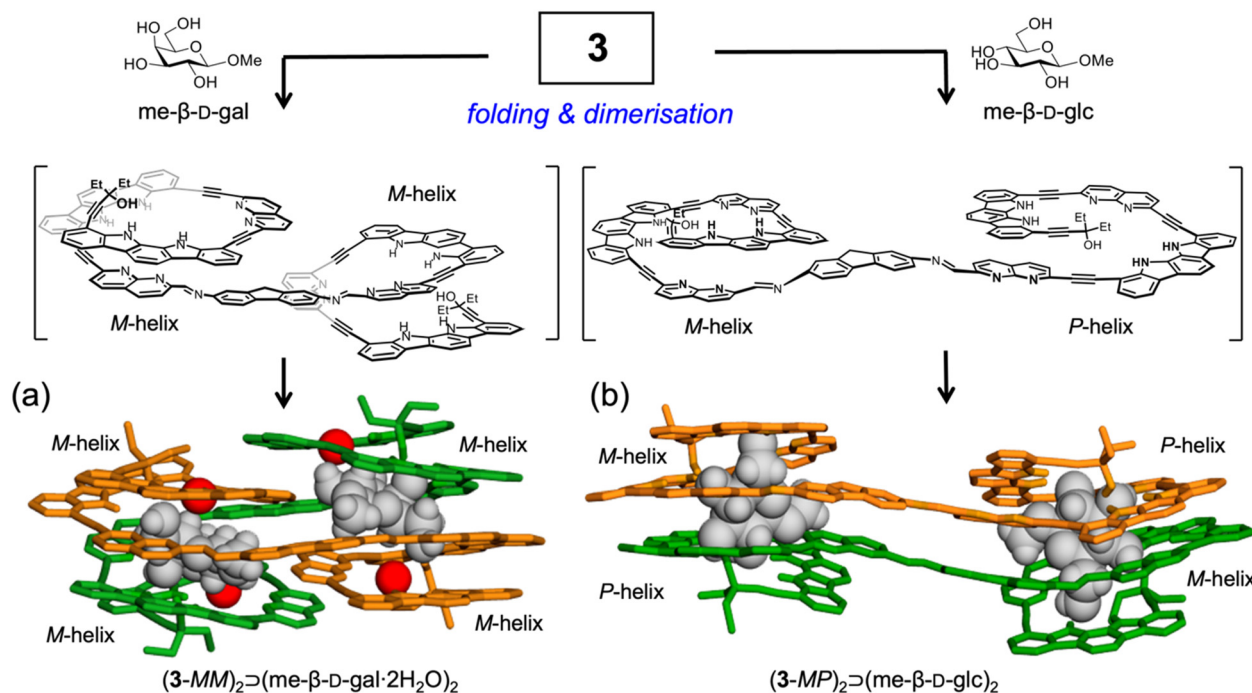†Electronic supplementary information (ESI) available: Synthetic protocols and characterisation new compounds and NMR spectra. See DOI: https://doi.org/10.1039/d4ob02061h

enabled us to quantitatively assemble synthetic receptors from its precursors through imine linkages, when a specific monosaccharide guest with strong affinity was present in solution. Specifically, foldameric receptor **3** was quantitatively assembled through imine bond formation between the aldehyde and amine precursors in the presence of methyl β-D-galactopyranoside (me-β-D-gal) or methyl β-D-glucopyranoside (me-β-D-glc) (Fig. 1). Both monosaccharides formed 2 : 2 receptor/guest complexes. However, the folding and assembly modes of receptor **3** in these complexes were quite different, featuring domain-swapping[7] cavities and guest-adaptive folding.[8] In the me-β-D-gal complex, the strand folded into a helical conformation with two identical half cavities in a trans-oid manner, adopting the same left-handed orientation (*M,M*). The two strands dimerised by stacking one half-cavity of a strand on top or below the other, generating two identical domain-swapping cavities, each encapsulating one me-β-D-gal with two water molecules (Fig. 1a). In contrast, in the me-β-D-glc complex, the strand adopted a folding structure with the two partial helices of opposite orientation: one left-handed (*M*) and one right-handed (*P*). In the *M*-helix, all four repeating monomers are fully folded. However, the *P*-helix is partially unfolded, with the naphthyridine monomer next to the imino linkage undergoing a 180° rotation. These two partial helices

This journal is © The Royal Society of Chemistry 2025

Org. Biomol. Chem., 2025, **23**, 2845–2853 | **2845**

Fig. 1 X-ray crystal structures of (a) (**3**-*MM*)₂ ⊃ (me-β-D-gal·2H₂O)₂ and (b) (**3**-*MP*)₂ ⊃ (me-β-D-glc)₂. me-β-D-gal: methyl β-D-galactopyranoside. me-β-D-glc: methyl β-D-glucopyranoside. Two separate strands are shown in green and orange tubes, and two guests and H₂O are shown in CPK views as grey and red, respectively. CH hydrogen atoms and *t*-butyls in **3** are omitted for clarity.[5]

were positioned in a cisoid mode around a central fluorene plane. The two strands were dimerised by face-to-face stacking in an antiparallel manner, which resulted in two binding cavities, each accommodating one molecule of me-β-D-glc (Fig. 1b).
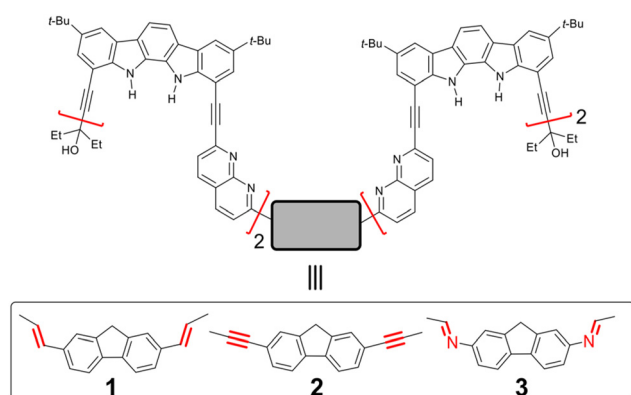
Despite the selective binding of specific monosaccharides, receptor **3** has limitations for potential applications in the transport, purification, and separation of monosaccharides in aqueous environments due to the chemical instability of the imine bond.[9] To overcome these limitations, we herein synthesised analogous foldameric receptors **1** and **2** by replacing the imine linkage with chemically stable ethenyl and ethynyl bonds, respectively (Scheme 1). These receptors were found to

provide nearly identical folding and binding properties to **3**, forming stable 2 : 2 receptor/guest complexes with methyl glycosides: (**1**-*MM*)₂ ⊃ (me-β-D-gal·2H₂O)₂ and (**1**-*MP*)₂ ⊃ (me-β-D-glc)₂ for receptor **1**, and (**2**-*MP*)₂ ⊃ (me-β-D-glc)₂ for receptor **2**. Furthermore, the more soluble receptor **2** in chlorinated solvents was used in U-tube transport experiments, showing the selective transport of me-β-D-glc over other glycosides.
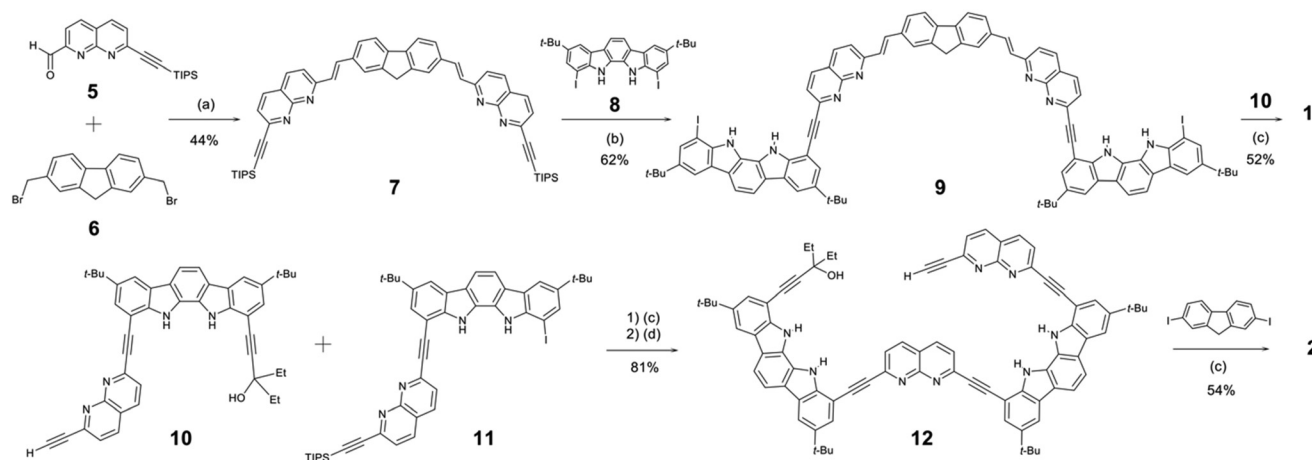
Results and discussion

The syntheses of receptors **1** and **2** are outlined in Scheme 2. The synthesis of compound **5** was described in ESI,† and the syntheses of compounds **6**,[10] **8**,[11] **10**,[12] and **11**[13] were previously reported. Compound **7** was synthesised by a PPh₃/NaH-mediated coupling reaction[14] between **5** (2.0 equiv.) and **6** (1.0 equiv.) in 44% yield. After protodesilylation with tetrabutyl-ammonium fluoride (TBAF), compound **7** was directly coupled with excess **8** (8 equiv.) to yield compound **9** in 62% yield. Subsequently, compound **9** was coupled with **10** (2.2 equiv.) to afford receptor **1** in 52% yield. On the other hand, a Pd (PPh₃)₂Cl₂/CuI-catalysed coupling reaction[15] between **10** and **11**, followed by protodesilylation with TBAF, gave compound **12** in 81% yield. Finally, compound **12** (2.1 equiv.) was coupled with 2,7-diiodo-9*H*-fluorene (1.0 equiv.) to yield receptor **2** in 54% yield.

As reported previously,[12,16] indolocarbazole-naphthyridine foldamers have a strong propensity to adopt helical conformations due to dipole–dipole interactions and π-stacking

Scheme 1 Chemical structures of foldameric receptors **1**, **2**, and **3**.

2846 | *Org. Biomol. Chem.*, 2025, **23**, 2845–2853

This journal is © The Royal Society of Chemistry 2025

Scheme 2 Syntheses of foldameric receptors **1** and **2**: (a) PPh$_3$, NaH, DMF, 40 °C; (b) CuI, Pd(PPh$_3$)$_2$Cl$_2$, TBAF (1.0 M in THF), DMF/TEA, 45 °C; (c) CuI, Pd(PPh$_3$)$_2$Cl$_2$, DMF/TEA, 45 °C; (d) TBAF (1.0 M in THF), THF, 25 °C.

between aromatic planes in CD$_2$Cl$_2$ and toluene-d_8. As a result, a tubular cavity is formed inside the aromatic helical backbone, where the indolocarbazole NHs and naphthyridine nitrogen atoms are located, allowing the binding of polyhydroxy guest molecules by the formation of multiple hydrogen bonds. Both receptors **1** and **2** contain two tetrameric units at the 2,7-positions of fluorene, which are spatially separated to form two independent helices. Each helical cavity is too small to fully encapsulate a monosaccharide, and therefore these receptors may assemble into dimers, forming larger cavities capable of encapsulating monosaccharides more effectively, as observed previously with receptor **3**.

The binding properties of receptor **1** with monosaccharides were investigated using ^{1}H NMR spectroscopy in 5% (v/v) DMSO-d_6/CD$_2$Cl$_2$, containing water (*ca.* 0.05%) (Fig. S1†). Upon the addition of me-β-D-gal to receptor **1**, a new separate set of ^{1}H NMR signals appeared (Fig. 2c and Fig. S17†), due to slow exchange between free **1** and its complex under the given conditions. As the amount of guest was gradually increased, this new set of signals intensified at the expense of free signals, without appearing any other sets of ^{1}H NMR signals for other possible complexes. Under these titration conditions, the signal intensities were saturated at an approximately 1 : 1 molar ratio of receptor **1** to me-β-D-gal. Upon complex formation, the CH signals of indolocarbazole (H11–H14 and H11*–H15*) were characteristically upfield-shifted (Δδ = 0.4–1.7 ppm) compared to those in free **1**. In addition, the naphthyridine CH signals (H9*, H17, H18*, and H19*) were upfield-shifted by Δδ = 0.7–1.2 ppm due to stacking between the aryl planes. Indolocarbazole NH signals split from four to eight peaks, and the OH signals of me-β-D-gal appeared in the downfield region between 10.5 and 6.1 ppm due to the formation of hydrogen bonds. Furthermore, ^{1}H–^{1}H ROESY experiment exhibited characteristic NOE cross-peaks between two different strands (*e.g.*, *t*-Bu4*-17, *t*-Bu4-16*, *t*-Bu3*-6, and *t*-Bu3-21*) (Fig. 2a, e and Fig. S6†). All these observations are consistent with an energy-minimised structure of a 2 : 2 stoi-

chiometric assembly, (**1**-*MM*)$_2$ ⊃ (me-β-D-gal·2H$_2$O)$_2$ (Fig. 2b and Fig. S5†).[17] It should be noted that the trends in splitting patterns and chemical shifts described above are nearly identical to those observed in the formation of complex (**3**-*MM*)$_2$ ⊃ (me-β-D-gal·2H$_2$O)$_2$, shown in Fig. 1. Additional evidence for the formation of a 2 : 2 complex between **1** and me-β-D-gal was obtained from diffusion ordered spectroscopy (DOSY). The diffusion coefficient for a 1 : 1 mixture of **1** and me-β-D-gal was estimated to be 3.0 × 10^{-10} m^2 s^{-1}, while that of **1** alone was 3.6 × 10^{-10} m^2 s^{-1} (Fig. 2d). Finally, ESI-MS also supported the formation of a 2 : 2 complex, showing characteristic peaks at *m/z* = 1867.9 ([[(**1**-*MM*)$_2$ ⊃ (me-β-D-gal·2H$_2$O)$_2$ + 2H + Na]$^{3+}$) and at *m/z* = 1869.2 ([[(**1**-*MM*)$_2$ ⊃ (me-β-D-gal·2H$_2$O)$_2$ + H + 2Na – H$_2$O]$^{3+}$) (Fig. 2f and Fig. S26†).

Similarly, the binding properties of receptor **1** with me-β-D-glc were examined using ^{1}H NMR spectroscopy in 5% (v/v) DMSO-d_6/CD$_2$Cl$_2$, containing water (*ca.* 0.05%). Upon the addition of me-β-D-glc at room temperature, a new separate set of ^{1}H NMR signals appeared. The intensities of these new signals were gradually increased at the expense of the original free signals, reaching saturation at a 1 : 1 molar ratio of receptor **1** to me-β-D-glc (Fig. 3c and Fig. S18†). It is noted that no ^{1}H NMR signals for other possible complexes were observed during the titration. Upon complex formation, significant upfield shifts (Δδ = 0.3–2.5 ppm) were observed in the CH signals of naphthyridine (H7*–H10* and H17–H20), fluorene (H21, H21*, and H22), and indolocarbazole (H2–H5) relative to those in free **1**. The OH signals of me-β-D-glc appeared between 10.9 to 8.1 ppm, indicative of hydrogen-bonding formation. Furthermore, ^{1}H–^{1}H ROESY experiment showed NOE correlations between the remote aromatic protons (*e.g.*, *t*-Bu2-21, *t*-Bu1-17, and 20-5) (Fig. S9†). The formation of a 2 : 2 complex between receptor **1** and me-β-D-glc was supported by DOSY experiments, which estimated a diffusion coefficient of 3.0 × 10^{-10} m^2 s^{-1} for a 1 : 1 mixture of **1** and me-β-D-glc, compared to 3.6 × 10^{-10} m^2 s^{-1} for **1** alone (Fig. S10†). Finally, ESI-MS spectra provided additional evidence, showing characteristic
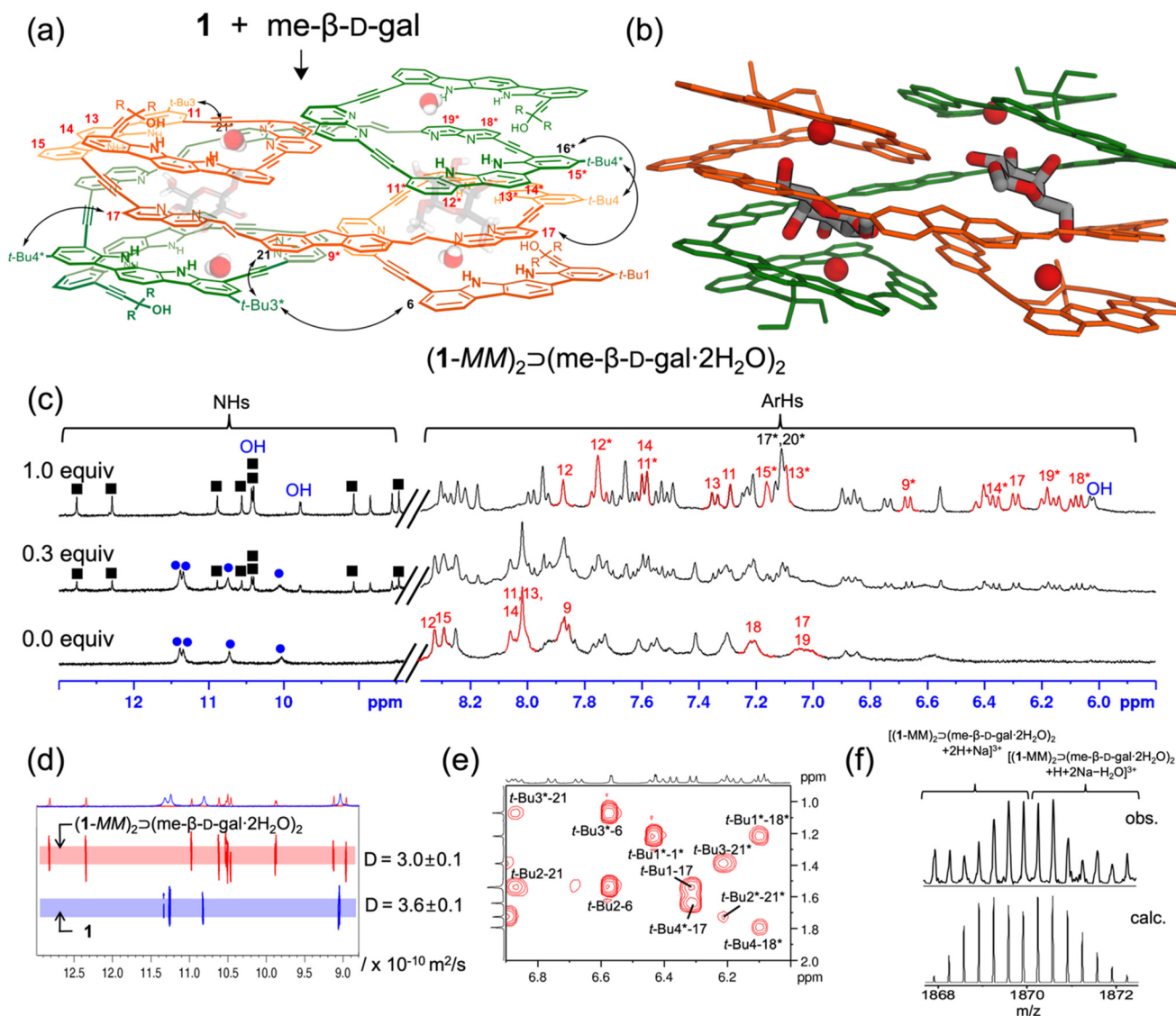
This journal is © The Royal Society of Chemistry 2025

Org. Biomol. Chem., 2025, **23**, 2845–2853 | **2847**

Fig. 2 (a) Possible molecular structure of complex $(1\text{-}MM)_2 \supset (\text{me-}\beta\text{-D-gal}\cdot 2H_2O)_2$ with NOE correlations (R = Et). (b) Energy-minimised structure of $(1\text{-}MM)_2 \supset (\text{me-}\beta\text{-D-gal}\cdot 2H_2O)_2$ (MacroModel 9.1, MMFFs force field, $CHCl_3$ phase). (c) Partial ^1H NMR spectra (400 MHz, 25 °C) of **1** (1.5 mM) with increasing me-β-D-gal in 5% (v/v) DMSO-d_6/CD_2Cl_2 at 25 °C. NH signals of **1** and its 2 : 2 complex are marked with blue circles and black squares, respectively. Helically stacked aromatic CH signals are depicted in red, and OH signals of me-β-D-gal are in blue. (d) Partial DOSY spectra (400 MHz, 25 °C) of **1** in the absence and presence of me-β-D-gal (2 mM) in 2% (v/v) DMSO-d_6/CD_2Cl_2. (e) Partial ^1H–^1H ROESY spectrum (400 MHz, 25 °C, mixing time 400 ms) of $(1\text{-}MM)_2 \supset (\text{me-}\beta\text{-D-gal}\cdot 2H_2O)_2$ (4 mM) in 2% (v/v) DMSO-d_6/CD_2Cl_2. (f) ESI-MS of a 2 : 2 complex: observed distribution (top) and calculated isotopic distribution (bottom) as $[(1\text{-}MM)_2 \supset (\text{me-}\beta\text{-D-gal}\cdot 2H_2O)_2 + 2H + Na]^{3+}$ and $[(1\text{-}MM)_2 \supset (\text{me-}\beta\text{-D-gal}\cdot 2H_2O)_2 + H + 2Na - H_2O]^{3+}$.

peaks at m/z = 1836.6 ($[(1\text{-}MP)_2 \supset (\text{me-}\beta\text{-D-glc})_2 + 3H]^{3+}$) and at m/z = 2754.3 ($[(1\text{-}MP)_2 \supset (\text{me-}\beta\text{-D-glc})_2 + 2H]^{2+}$) (Fig. 3b and Fig. S26†). All these observations confirm the formation of a 2 : 2 complex between **1** and me-β-D-glc.

However, ^1H NMR spectra showed clear differences between the two complexes, me-β-D-glc and me-β-D-gal complexes. In the me-β-D-glc complex, the CH signals of fluorene (H24, H24*) and naphthyridine (H7*, H10*, and H17–H20) were more upfield-shifted by 0.7–2.4 ppm compared to the me-β-D-gal complex. Conversely, the indolocarbazole (H11–H13, H12*–H15*) were downfield-shifted by $\Delta\delta$ = 0.3–1.2 ppm in the

me-β-D-glc complex. In addition, ^1H–^1H ROESY experiment revealed characteristic NOE cross-peaks (t-Bu4*-21, t-Bu3*-17, and t-Bu2*-8) that are absent in the me-β-D-gal complex (Fig. 3a and Fig. S9†). Furthermore, circular dichroism (CD) intensities between the two complexes were considerably different from each other. Receptor **1** was CD-inactive in 5% (v/v) DMSO/CH_2Cl_2 (Fig. 4 and Fig. S16†). Upon the addition of me-β-D-gal and me-β-D-glc, induced CD signals were observed, indicating the bias of helical handedness in the resulting complexes. Specifically, the CD intensity of the me-β-D-gal complex was $\Delta\varepsilon_{(475\text{ nm})}$ = −134.7 M^{-1} cm^{-1}, while that of the me-β-D-glc
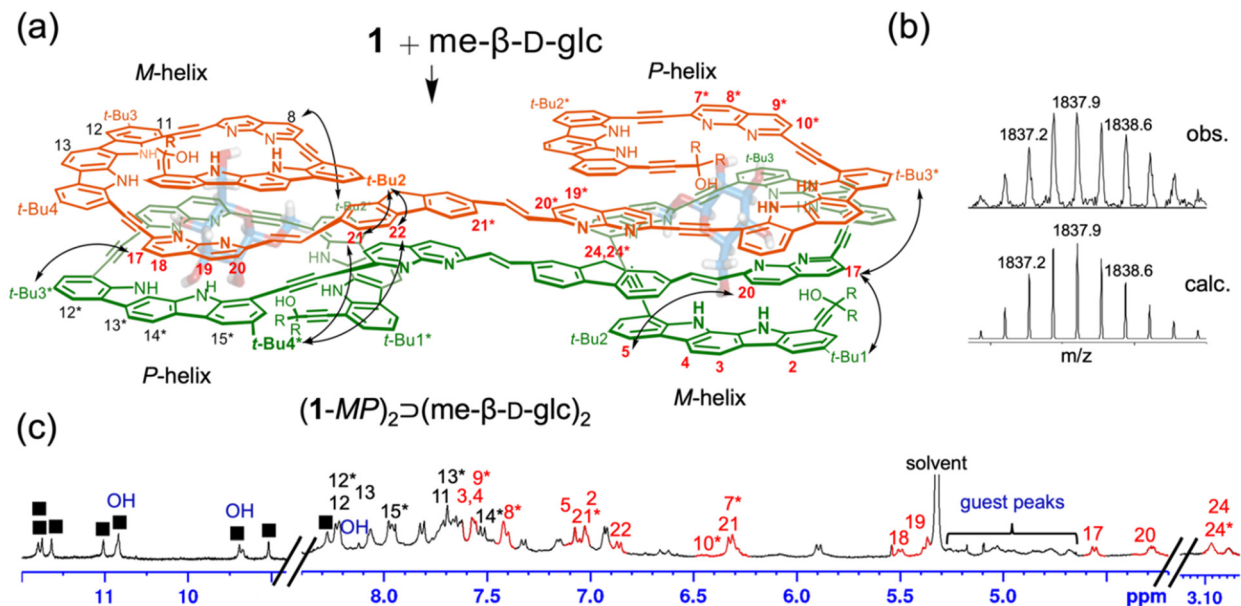
2848 | *Org. Biomol. Chem.*, 2025, **23**, 2845–2853

This journal is © The Royal Society of Chemistry 2025

Fig. 3 (a) Possible molecular structure of (**1**-*MP*)$_2$ ⊃ (me-β-D-glc)$_2$ with NOE correlations (R = Et). (b) ESI-MS of the 2 : 2 complex: observed distribution (top) and calculated isotopic distribution (bottom) as [(**1**-*MP*)$_2$ ⊃ (me-β-D-glc)$_2$ + 3H]$^{3+}$. (c) Partial ^{1}H NMR spectrum (400 MHz, 25 °C) of **1** (2.0 mM) after adding me-β-D-glc (1 equiv.) in 5% (v/v) DMSO-d_6/CD$_2$Cl$_2$ at 25 °C. NH signals of complex are marked with black squares. Helically stacked aromatic CH signals are depicted in red, and OH signals of me-β-D-glc are in blue.

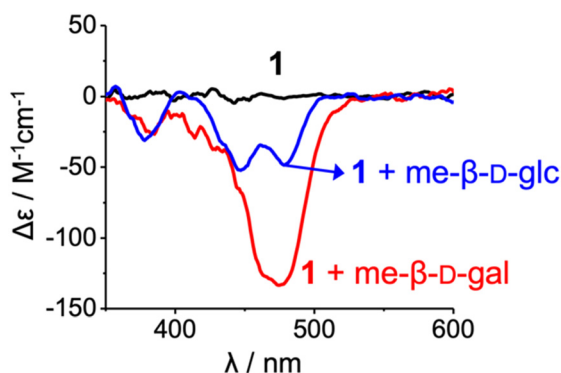**Fig. 4** CD spectra of **1** (2.00 × 10^{-5} M, 25 ± 1 °C) and their complexes with me-β-D-gal and me-β-D-glc (*ca.* 200 equiv.) in 5% (v/v) DMSO/CH$_2$Cl$_2$.

complex was much smaller, only Δε$_{(446 \text{ nm})}$ = −51.5 M^{-1} cm^{-1} and Δε$_{(478 \text{ nm})}$ = −47.7 M^{-1} cm^{-1}. These results are nearly identical to those observed with receptor **3**, strongly suggesting that receptor **1** adopts (*M*,*M*)-helices in the me-β-D-gal complex but (*M*,*P*)-helices of a pseudo-*meso* type in the me-β-D-glc complex (for an energy-minimised structure, see Fig. S8†)[17]

The quantitative binding properties of receptor **1** with me-β-D-gal and me-β-D-glc were investigated using isothermal titration calorimetry (ITC) in 5% (v/v) DMSO/CH$_2$Cl$_2$ (containing *ca.* 0.05% water, 22 °C) (Fig. S20, S21 and Tables S4, S5†). As mentioned in the ^{1}H NMR studies, only signals corresponding to 2 : 2 complexes between **1** and these guests were observed throughout the titrations. No signals for possible 1 : 1, 1 : 2, and 2 : 1 complexes were detected. Therefore, the binding con-

stants were calculated under the assumption that 2 : 2 complexes formed through a single step, as shown in eqn (1).

$$2 \text{ receptor} + 2 \text{ guest} \rightleftharpoons (\text{receptor})_2 \cdot (\text{guest})_2$$
$$K = \frac{[\text{receptor}_2 \cdot \text{guest}_2]}{[\text{receptor}]^2 [\text{guest}]^2} \quad (1)$$

The ITC experiments also support this assumption, showing sigmoidal curves with single inflection points at molar ratios of approximately 1 (**1**/guest). The binding curves were analysed using HypCal software,[18] and the association constants (log *K*) for the 2 : 2 complexes were estimated to be 12.7 for me-β-D-gal and 13.3 for me-β-D-glc. Although their comparable binding affinities, the two complexes exhibited very different thermodynamic parameters. For the me-β-D-gal complex, the enthalpy (Δ*H*°) and entropy (*T*Δ*S*°) values were −117.0 kJ mol^{-1} and −45.4 kJ mol^{-1}, respectively. In contrast, the values for the me-β-D-glc complex were Δ*H*° = −55.0 kJ mol^{-1} and *T*Δ*S*° = +20.3 kJ mol^{-1} (Table 1). These differences are possibly

Table 1 ITC experiment results for receptors **1** and **2** in 5% (v/v) DMSO/CH$_2$Cl$_2$ (containing *ca.* 0.05% water) at 22 °C

Receptor	Guest	Log *K* (2 : 2 complex)	Δ*G*° (kJ mol^{-1})	Δ*H*°	*T*Δ*S*°
1	me-β-D-gal	12.7 ± 0.1	−71.6	−117.0	−45.4
	me-β-D-glc	13.3 ± 0.1	−75.3	−55.0	+20.3
	me-α-D-glc	10.9 ± 0.1	−61.4	−36.4	+25.0
2	me-β-D-gal	11.1 ± 0.1	−62.6	−80.3	−17.7
	me-β-D-glc	13.9 ± 0.1	−78.3	−51.1	+27.2
	me-α-D-glc	10.6 ± 0.1	−60.1	−48.6	+11.5

This journal is © The Royal Society of Chemistry 2025

Org. Biomol. Chem., 2025, **23**, 2845–2853 | **2849**

attributed to the presence of water molecules contained in the 2 : 2 complexes, as observed in the complexes between receptor **3** and these guests (Fig. 1). The me-β-D-gal complex may include four water molecules but no water molecules are involved in the me-β-D-glc complex, as supported by their ESI-mass spectra. Under the titration conditions containing approximately 0.05% water, several water molecules are present in the internal cavities of free receptor **1** through hydrogen-bonding interactions, as seen in the X-ray structures of an indolocarbazole-naphthyridine folda-

mer.[16] Some or all of these water molecules are likely released upon guest binding. The thermodynamic parameters indicate that the me-β-D-gal complex is enthalpically more favourable while the me-β-D-glc complex is entropically more favourable. This result is consistent with the fact that water molecules are partially liberated in the former complex but completely liberated in the latter complex.

Next, the binding properties of receptor **2** with monosaccharides were investigated using ^{1}H NMR spectroscopy in 5%
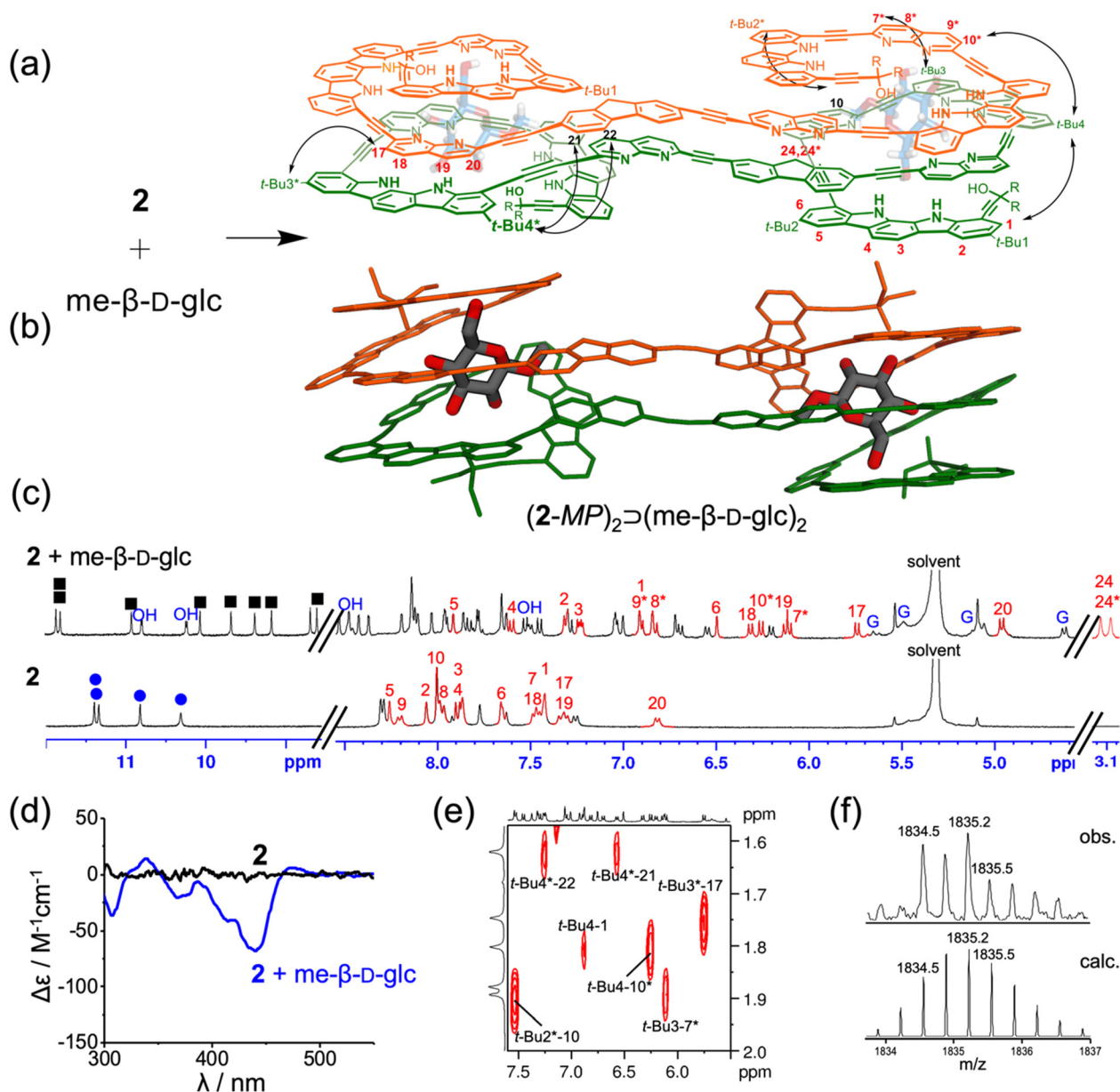

Fig. 5 (a) Possible molecular structure of (**2**-*MP*)$_2$ ⊃ (me-β-D-glc)$_2$ with NOE correlations (R = Et). (b) Energy-minimised structure of (**2**-*MP*)$_2$ ⊃ (me-β-D-glc)$_2$ (MacroModel 9.1, MMFFs force field, CHCl$_3$ phase). (c) Partial ^{1}H NMR spectra (400 MHz, 25 °C) of **2** (1.5 mM) in the absence and presence of me-β-D-glc (1.0 equiv.) in 5% (v/v) DMSO-d_6/CD$_2$Cl$_2$. Helically stacked CH signals are depicted in red, and me-β-D-glc signals are in blue. The blue circles and black squares correspond to the NH signals of free **2** and its 2 : 2 complex. (d) CD spectra of **2** (2.00 × 10^{-5} M, 25 ± 1 °C) and its complex with me-β-D-glc in 5% (v/v) DMSO/CH$_2$Cl$_2$. (e) Partial ^{1}H–^{1}H ROESY spectrum (400 MHz, 25 °C, mixing time 400 ms) of (**2**-*MP*)$_2$ ⊃ (me-β-D-glc)$_2$ (4 mM) in CD$_2$Cl$_2$. (f) ESI-MS of the 2 : 2 complex: observed distribution (top) and calculated isotopic distribution (bottom) as [(**2**-*MP*)$_2$ ⊃ (me-β-D-glc)$_2$ + 3H]$^{3+}$.
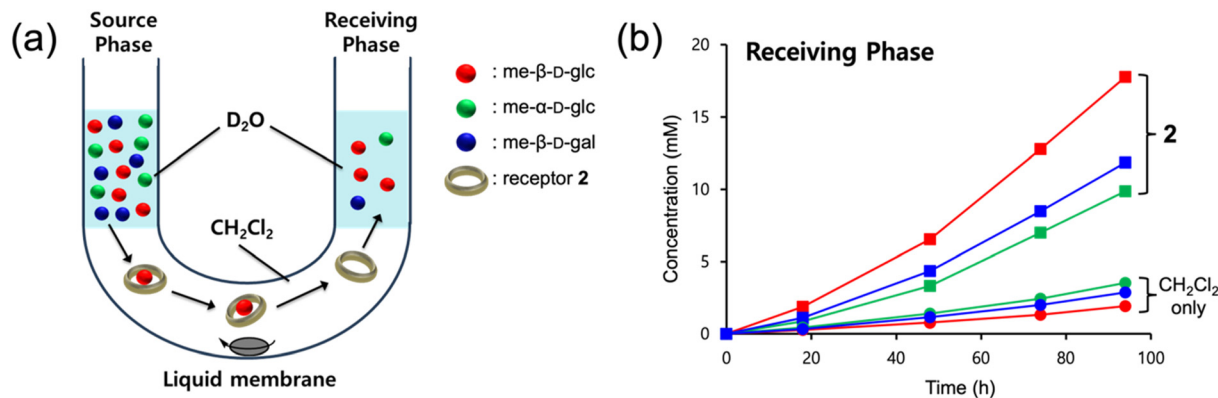
2850 | *Org. Biomol. Chem.*, 2025, **23**, 2845–2853

This journal is © The Royal Society of Chemistry 2025

Fig. 6 (a) Cartoon representation of the U-tube experiment. (b) Time-dependent concentration profiles of me-β-D-glc (red), of me-α-D-glc (green), and me-β-D-gal (blue) in receiving phase, in the absence and presence of receptor **2** in liquid membrane. Source phase (0.7 mL D$_2$O, [me-β-D-glc] = [me-α-D-glc] = [me-β-D-gal] = 2.0 M); liquid membrane (2 mL, CH$_2$Cl$_2$, [**2**] = 3.0 mM); receiving phase (0.7 mL D$_2$O), 10 °C.

(v/v) DMSO-d_6/CD$_2$Cl$_2$ containing water (*ca.* 0.05%) (Fig. S2†). Interestingly, receptor **2** showed a well-resolved ^{1}H NMR spectrum only when complexed with me-β-D-glc, while broad, unresolved spectra were observed in the presence of other guests (me-β-D-gal, me-α-D-glc, me-α-D-gal, and me-α-D-man). The addition of me-β-D-glc to **2** resulted in the splitting of NH signals, from four to eight (Fig. 5c and Fig. S19†). Moreover, the CH signals of indolocarbazole (H1–H6), naphthyridine (H7*–H10*, H17–H20), and fluorene (H24, H24*) are noticeably upfield-shifted (Δδ = 0.3–1.8 ppm) due to aromatic stacking interactions between the aryl planes. All OH signals of me-β-glc were largely downfield-shifted (δ = 10.9–7.5 ppm) as a result of the formation of strong hydrogen bonds. Furthermore, [1]H–[1]H ROESY experiments revealed NOE correlations between the two different strands (*t*-Bu4*-21, *t*-Bu3*-17, *t*-Bu3-7*, and *t*-Bu2*-10) (Fig. 5a, e and Fig. S14†). All these results were consistent with an energy-minimised structure of (**2**-*MP*)$_2$ ⊃ (me-β-D-glc)$_2$ (Fig. 5b and Fig. S13†).[17] As anticipated, CD spectroscopy of **2** exhibited a low induced negative Cotton effects (Δε$_{(439 \text{ nm})}$ = −66.8 M^{-1} cm^{-1}) upon the addition of me-β-D-glc, further supporting pseudo-*meso* conformation of (**2**-*MP*)$_2$ ⊃ (me-β-D-glc)$_2$ (Fig. 5d and Fig. S16†). Finally, ESI-MS spectra also showed 2 : 2 complex peaks at *m/z* = 1833.9 ([(**2**-*MP*)$_2$ ⊃ (me-β-D-glc)$_2$ + 3H]$^{3+}$) and at *m/z* = 2750.3 ([(**2**-*MP*)$_2$ ⊃ (me-β-D-glc)$_2$ + 2H]$^{2+}$) (Fig. 5f and Fig. S27†).

The binding affinities of receptor **2** for monosaccharides were measured and compared using isothermal titration calorimetry (ITC) in 5% (v/v) DMSO/CH$_2$Cl$_2$ (containing *ca.* 0.05% water, 22 °C) (Fig. S23–S25 and Tables S7–S9†). For the formation of a 2 : 2 complex between **2** and me-β-D-glc, the association constant (log *K*) was estimated to be 13.9, with Δ*H*° = −51.1 kJ mol^{-1} and *T*Δ*S*° = +27.2 kJ mol^{-1} (Table 1). These values were nearly identical to the 2 : 2 complex formation between **1** and me-β-D-glc, further supporting the formation of (**2**-*MP*)$_2$ ⊃ (me-β-D-glc)$_2$. Under the same conditions, the association constants (log *K*) were calculated to be 11.1 for me-β-D-gal and 10.6 for me-α-D-glc, both of which are two to three orders of magnitudes weaker than that for me-β-D-glc. These weaker

affinities are likely responsible for the unresolved and broad ^{1}H NMR spectra of their complexes under the given conditions.

Finally, we performed liquid–liquid transport experiments using a U-tube apparatus to investigate whether receptors **1** and **2** could facilitate the transport of monosaccharides across an organic solvent layer.[19] However, receptor **1** was not suitable for the transport experiment due to the low solubility in chlorinated solvents, and the experiments were conducted with the more soluble receptor **2**. As depicted in Fig. 6a, a source phase of D$_2$O containing a mixture of me-β-D-glc, me-β-D-gal, and me-α-D-glc (2.0 M of each) and a receiving D$_2$O phase were placed on opposite sides of a CH$_2$Cl$_2$ liquid membrane with or without receptor **2** (3.0 mM). A stirring bar was positioned at the bottom of the CH$_2$Cl$_2$ phase, and the system was stirred at 10 °C. The amount of transported guests was quantified by integrating the ^{1}H NMR signals relative to DMSO (2 mM in D$_2$O) used as an external standard (Fig. S15†). As a result, the presence of **2** in the CH$_2$Cl$_2$ layer significantly enhanced the transport of monosaccharides from the source phase to the receiving phase. Specifically, the concentration of me-β-D-glc in the receiving phase reached 17.8 mM in the presence of **2** after 96 h, compared to only 1.8 mM in its absence under the same conditions. Furthermore, the selective transport of me-β-D-glc over me-β-D-gal and me-α-D-glc was shown (Fig. 6b). The observed trend in transport efficiency is in parallel with their binding affinities.

Conclusions

In this study, we present foldameric receptors **1** and **2** which adopt helical conformations and assemble to generate domain-swapping cavities for monosaccharides. Comprehensive analysis using ^{1}H NMR, ESI-mass, CD spectroscopy, and ITC experiments revealed that receptor **1** forms two distinct 2 : 2 receptor/guest complexes: (**1**-*MM*)$_2$ ⊃ (me-β-D-gal·2H$_2$O)$_2$ and (**1**-*MP*)$_2$ ⊃ (me-β-D-glc)$_2$, exhibiting different

This journal is © The Royal Society of Chemistry 2025

Org. Biomol. Chem., 2025, **23**, 2845–2853 | **2851**

folding and assembly modes for optimal stability. In contrast, receptor **2** forms a single stable 2 : 2 complex, (**2**-*MP*)$_2$ ⊃ (me-β-D-glc)$_2$, with significantly stronger binding affinity for me-β-D-glc compared to other methyl glycoside guests. U-tube transport experiments showed that receptor **2** selectively transports me-β-D-glc across an organic phase (CH$_2$Cl$_2$). This study clearly demonstrates that aromatic foldamers can serve as versatile synthetic receptors, with the right balance between rigidity and flexibility, enabling adaptive folding and assembly, thereby optimising the binding and transport of specific guests. Furthermore, the modification of the repeating units and sequences could enable the development of foldameric receptors capable of binding and transporting other saccharides.

Experimental section

Receptor 1

A yellow solid; mp > 275 °C (dec); ^{1}H NMR (400 MHz, DMSO-d_6, 25 °C, ppm) δ 11.63 (s, 1H), 11.45 (s, 1H), 11.38 (s, 1H), 10.74 (s, 1H), 8.57 (d, J = 8.4 Hz, 1H), 8.45 (s, 1H), 8.43 (s, 1H), 8.35 (d, J = 1.4 Hz, 1H), 8.35 (d, J = 8.3 Hz, 1H), 8.18 (d, J = 1.4 Hz, 1H), 8.14 (s, 4H), 8.01 (d, J = 8.3 Hz, 1H), 7.96 (d, J = 8.4 Hz, 1H), 7.88 (d, J = 8.3 Hz, 1H), 7.94 (d, J = 1.5 Hz, 1H), 7.82 (s, 1H), 7.80 (d, J = 7.5 Hz, 1H), 7.79 (d, J = 8.3 Hz, 1H), 7.76 (d, J = 8.2 Hz, 1H), 7.68 (d, J = 16.1 Hz, 1H), 7.66 (d, J = 1.4 Hz, 1H), 7.63 (s, 1H), 7.45 (d, J = 7.5 Hz, 1H), 7.43 (d, J = 1.6 Hz, 1H), 7.31 (d, J = 8.3 Hz, 1H), 7.21 (d, J = 16.2 Hz, 1H), 5.18 (s, OH), 3.70 (s, 1H), 1.75–1.62 (m, 4H), 1.50 (s, 18H, *t*-Bu), 1.44 (s, 9H, *t*-Bu), 1.38 (s, 9H, *t*-Bu), 0.98 (t, J = 7.3 Hz, 6H); ^{13}C NMR (100 MHz, DMSO-d_6, 25 °C, ppm) δ 158.9, 155.3, 155.2, 146.7, 145.7, 143.9, 142.2, 142.1, 141.8, 141.7, 141.5, 138.0, 137.9, 137.8, 137.1, 134.7, 127.1, 126.3, 126.0, 125.9, 125.9, 125.8, 125.7, 124.2, 124.1, 123.7, 121.2, 120.8, 120.7, 120.6, 120.4, 119.1, 118.8, 116.7, 112.5, 112.3, 112.1, 105.0, 103.2, 102.9, 97.5, 93.2, 93.1, 92.9, 89.4, 89.0, 87.9, 79.7, 70.9, 34.5, 34.4, 34.3, 33.8, 31.7, 31.6, 29.0, 20.7, 8.7; ESI-HRMS, *m/z* calcd for C$_{179}$H$_{154}$N$_{16}$O$_2$ [M + 2H]$^{2+}$ 1280.6293 found 1280.6277.

Receptor 2

A yellow solid; mp > 265 °C (dec); ^{1}H NMR (400 MHz, DMSO-d_6, 25 °C, ppm) δ 11.56 (s, 1H), 11.44 (s, 2H), 10.78 (s, 1H), 8.61 (d, J = 8.4 Hz, 1H), 8.47 (d, J = 8.4 Hz, 1H), 8.43 (s, 1H), 8.42 (s, 1H), 8.38 (d, J = 1.5 Hz, 1H), 8.21 (d, J = 8.4 Hz, 1H), 8.18 (d, J = 1.6 Hz, 1H), 8.11 (d, J = 8.4 Hz, 1H), 8.47 (s, 2H), 8.04 (d, J = 8.3 Hz, 1H), 7.98 (d, J = 8.3 Hz, 1H), 7.98 (d, J = 8.3 Hz, 1H), 7.89 (d, J = 8.3 Hz, 1H), 7.86 (d, J = 8.3 Hz, 1H), 7.83 (d, J = 7.5 Hz, 1H), 7.83 (d, J = 1.5 Hz, 1H), 7.81 (d, J = 1.6 Hz, 1H), 7.72 (d, J = 1.6 Hz, 1H), 7.66 (s, 1H), 7.44 (d, J = 1.6 Hz, 1H), 7.42 (d, J = 7.5 Hz, 1H), 7.29 (d, J = 8.3 Hz, 1H), 5.21 (s, OH), 3.78 (s, 1H), 1.76–1.64 (m, 4H), 1.49 (s, 18H, *t*-Bu), 1.43 (s, 9H, *t*-Bu), 1.37 (s, 9H, *t*-Bu), 1.00 (t, J = 7.3 Hz, 6H); ^{13}C NMR (100 MHz, DMSO-d_6, 25 °C, ppm) δ 155.8, 155.5, 147.3, 147.2, 146.9, 146.7, 144.2, 142.7, 142.6, 142.4, 142.2, 142.0, 138.6, 138.4, 138.4, 138.3, 138.2, 137.9, 137.6, 131.4, 129.0, 126.9, 126.5, 126.4, 126.4, 126.2, 125.5, 124.7, 124.6, 124.6, 124.2, 121.8, 121.4, 121.3, 121.2, 121.1, 120.9, 120.0, 119.5, 119.4, 117.2, 113.1, 112.8, 112.6, 105.4, 103.4, 103.4, 103.3, 98.0, 93.6, 93.4, 92.1, 90.1, 90.0, 89.5, 89.3, 80.1, 71.4, 35.0, 34.9, 34.8, 34.3, 33.7, 32.2, 32.1, 23.1, 15.2, 9.2; ESI-HRMS, *m/z* calcd for C$_{179}$H$_{150}$N$_{16}$O$_2$ [M + 2H]$^{2+}$ 1278.6137 found 1278.6130.

NMR titrations

A solvent mixture of 5% (v/v) DMSO-d_6/CD$_2$Cl$_2$ with water content of *ca.* 0.05% was prepared using dried DMSO-d_6 and a 10 : 1 (v/v) mixture of anhydrous and water-saturated CH$_2$Cl$_2$. Organic solvents were dried over molecular sieves (4 Å). Water-saturated CD$_2$Cl$_2$ was prepared by sonicating the CD$_2$Cl$_2$ with a few drops of distilled water for 20 min, followed by carefully separating the organic layer. Stock solution of **1** and **2** (1.50 mM), and each guest (6.00 mM) were prepared separately using this solvent mixture. A 400 µL of the **1** and **2** solution was taken in a NMR tube and an initial spectrum was taken to determine the chemical shifts of free receptors. Aliquots of the guest solution were added to the NMR tube and the spectrum was recorded after each addition.

ITC experiments

Stock solutions of receptors **1** and **2** (0.09–0.30 mM) and each guest (4.00–7.00 mM) were prepared separately in 5% (v/v) DMSO/CH$_2$Cl$_2$ (containing *ca.* 0.05% water). ITC experiments were conducted by adding the solution of receptor to the ITC sample cell, followed by adding each solution of a guest using a syringe. Heats of dilution which was obtained by titrating each guest into the ITC sample cell in the absence of receptors were subtracted. ITC experiments were recorded using MicroCal VP-ITC (spacing time: 240 s, temperature: 22 °C, injection volume: 3 or 4 µL). Thermodynamic values were determined using HypCal software[18] based on eqn (1).

U-tube transport experiments

Stock solutions of a source phase containing a mixture of me-β-D-glc, me-β-D-gal, and me-α-D-glc (2.0 M of each) in D$_2$O and receptor **2** (3.0 mM) in CH$_2$Cl$_2$ were prepared separately. A U-tube apparatus with an internal diameter of 0.4 cm, a height of 7.8 cm, and a 3.0 cm distance between the two arms was used. For the experiment, 0.7 mL of the D$_2$O source phase and 0.7 mL of the receiving D$_2$O phase were placed on opposite sides of the U-tube, with 2.0 mL of the receptor **2** solution in CH$_2$Cl$_2$ placed in the middle. A stirring bar was positioned at the bottom of the CH$_2$Cl$_2$ phase, and the system was stirred at 500 rpm at 10 °C. The background experiment was performed under identical conditions without receptor **2**. The amount of transported guests was quantified by integrating the ^{1}H NMR signals relative to DMSO (2.0 mM in D$_2$O) used as an external reference.

Author contributions

G. S. performed all experiments and data analysis. K.-S. J. conceived and supervised the project. All authors discussed the results and write, read, and reviewed the manuscript.

2852 | *Org. Biomol. Chem.*, 2025, **23**, 2845–2853

This journal is © The Royal Society of Chemistry 2025

Data availability

The data supporting this article are included in the ESI.†

Conflicts of interest

There are no conflicts to declare.

Acknowledgements

References

1 (a) H. G. Garg, M. K. Cowman and C. A. Hales, *Carbohydrate Chemistry, Biology and Medical Applications*, Elsevier, Amsterdam, 2008; (b) H. M. Asif, M. Akram, T. Saeed, M. I. Khan, N. Akhtar, R. ur Rehman, S. M. A. Shah, K. Ahmed and G. Shaheen, *Int. Res. J. Biochem. Bioinform.*, 2011, **1**, 1–5; (c) G. A. Rabinovich, Y. van Kooyk and B. A. Cobb, *Ann. N. Y. Acad. Sci.*, 2012, **1253**, 1–15; (d) M. He, X. Zhou and X. Wang, *Sig. Transduct. Target. Ther.*, 2024, **9**, 194.

2 (a) M. Mazik, *Chem. Soc. Rev.*, 2009, **38**, 935–956; (b) X. Sun and T. D. James, *Chem. Rev.*, 2015, **115**, 8001–8037; (c) A. P. Davis, *Chem. Soc. Rev.*, 2020, **49**, 2531–2545; (d) R. Ahamed, J. Venkatesh, R. Srithar, S. Gaikwad and S. Pramanik, *Org. Biomol. Chem.*, 2023, **21**, 5492–5505; (e) X. Sun, B. M. Chapin, P. Metola, B. Collins, B. Wang, T. D. James and E. V. Anslyn, *Nat. Chem.*, 2019, **11**, 768–778; (f) B. Wu, R. Tang and Y. Tan, *Nat. Rev. Chem.*, 2025, **9**, 10–27.

3 (a) Y. Ferrand, M. P. Crump and A. P. Davis, *Science*, 2007, **318**, 619–622; (b) N. Chandramouli, Y. Ferrand, G. Lautrette, B. Kauffmann, C. D. Mackereth, M. Laguerre, D. Dubreuil and I. Huc, *Nat. Chem.*, 2015, **7**, 334–341; (c) R. A. Tromans, T. S. Carter, L. Chabanne, M. P. Crump, H. Li, J. V. Matlock, M. G. Orchard and A. P. Davis, *Nat. Chem.*, 2019, **11**, 52–56; (d) B. J. J. Timmer, A. Kooijman, X. Schaapkens and T. J. Mooibroek, *Angew. Chem., Int. Ed.*, 2021, **60**, 16178–16183; (e) J. K. Awino, R. W. Gunasekara and Y. Zhao, *J. Am. Chem. Soc.*, 2016, **138**, 9759–9762; (f) R. W. Gunasekara and Y. Zhao, *J. Am. Chem. Soc.*, 2017, **139**, 829–835; (g) X. Li and Y. Zhao, *Chem. Sci.*, 2021, **12**, 374–383.

4 (a) A. P. Davis and R. S. Wareham, *Angew. Chem., Int. Ed.*, 1999, **38**, 2978–2996; (b) S. Tommasone, F. Allabush, Y. K. Tagger, J. Norman, M. Köpf, J. H. R. Tucker and P. M. Mendes, *Chem. Soc. Rev.*, 2019, **48**, 5488–5505.

5 G. Song, S. Lee and K.-S. Jeong, *Nat. Commun.*, 2024, **15**, 1501.

6 (a) J.-F. Ayme, J. E. Beves, D. A. Leigh, R. T. McBurney, K. Rissanen and D. Schultz, *Nat. Chem.*, 2012, **4**, 15–20; (b) C. G. Pappas, P. K. Mandal, B. Liu, B. Kauffmann, X. Miao, D. Komáromy, W. Hoffmann, C. Manz, R. Chang, K. Liu, K. Pagel, I. Huc and S. Otto, *Nat. Chem.*, 2020, **12**, 1180–1186; (c) D. Yang, L. K. S. von Krbek, L. Yu, T. K. Ronson, J. D. Thoburn, J. P. Carpenter, J. L. Greenfield, D. J. Howe, B. Wu and J. R. Nitschke, *Angew. Chem., Int. Ed.*, 2021, **60**, 4485–4490; (d) N. M. A. Speakman, A. W. Heard and J. R. Nitschke, *J. Am. Chem. Soc.*, 2024, **146**, 10234–10239.

7 (a) N. Nandwani, P. Surana, H. Negi, N. M. Mascarenhas, J. B. Udgaonkar, R. Das and S. Gosavi, *Nat. Commun.*, 2019, **10**, 452; (b) S. Wang, B. Wicher, C. Douat, V. Maurizot and I. Huc, *Angew. Chem., Int. Ed.*, 2024, **63**, e202405091.

8 (a) L.-P. Yang, F. Jia, Q.-H. Zhou, F. Pan, J.-N. Sun, K. Rissanen, L. W. Chung and W. Jiang, *Chem. – Eur. J.*, 2017, **23**, 1516–1520; (b) S. H. Yoo, J. Buratto, A. Roy, E. Morvane, M. Pasco, K. Pulka-Ziach, C. M. Lombardo, F. Rosu, V. Gabelica, C. D. Mackereth, G. W. Collie and G. Guichard, *J. Am. Chem. Soc.*, 2022, **144**, 15988–15998.

9 M. E. Belowich and J. F. Stoddart, *Chem. Soc. Rev.*, 2012, **41**, 2003–2024.

10 D. Wang, M. V. Ivanov, D. Kokkin, J. Loman, J.-Z. Cai, S. A. Reid and R. Rathore, *Angew. Chem., Int. Ed.*, 2018, **57**, 8189–8193.

11 K.-J. Chang, D. Moon, M. S. Lah and K.-S. Jeong, *Angew. Chem., Int. Ed.*, 2005, **44**, 7926–7929.

12 K. M. Kim, G. Song, S. Lee, H.-G. Jeon, W. Chae and K.-S. Jeong, *Angew. Chem., Int. Ed.*, 2020, **59**, 22475–22479.

13 G. Song and K.-S. Jeong, *ChemPlusChem*, 2020, **85**, 2475–2481.

14 (a) B. E. Maryanoff and A. B. Reitz, *Chem. Rev.*, 1989, **89**, 863–927; (b) P. A. Byrne and D. G. Gilheany, *Chem. Soc. Rev.*, 2013, **42**, 6670–6696.

15 (a) K. Sonogashira, Y. Tohda and N. Hagihara, *Tetrahedron Lett.*, 1975, **16**, 4467–4470; (b) R. Chinchilla and C. Nájera, *Chem. Rev.*, 2007, **107**, 874–922.

16 (a) J. Y. Hwang, H.-G. Jeon, Y. R. Choi, J. Kim, P. Kang, S. Lee and K.-S. Jeong, *Org. Lett.*, 2017, **19**, 5625–5628; (b) G. Song, K. M. Kim, S. Lee and K.-S. Joeng, *Chem. – Asian J.*, 2021, **16**, 2958–2966.

17 (a) F. Mohamadi, N. G. J. Richards, W. C. Guida, R. Liskamp, M. Lipton, C. Caufield, G. Chang, T. Hendrickson and W. C. Still, *J. Comput. Chem.*, 1990, **11**, 440–467; (b) T. A. Halgren, *J. Comput. Chem.*, 1996, **17**, 490–519.

18 (a) HypCal program in Hyperquad; (b) G. Arena, P. Gans and C. Sgarlata, *Anal. Bioanal. Chem.*, 2016, **408**, 6413–6422.

19 (a) T. Kida, T. Ohe, H. Higashimoto, H. Harada, Y. Nakatsuji, I. Ikeda and M. Akashi, *Chem. Lett.*, 2004, **33**, 258–259; (b) H. Abe, T. Yoneda, Y. Ohishi and M. Inouye, *Chem. – Eur. J.*, 2016, **22**, 18944–18952; (c) Q. He, G. M. Peters, V. M. Lynch and J. L. Sessler, *Angew. Chem., Int. Ed.*, 2017, **56**, 13396–13400; (d) A. Docker, I. Marques, H. Kuhn, Z. Zhang, V. Félix and P. D. Beer, *J. Am. Chem. Soc.*, 2022, **144**, 14778–14789.

This journal is © The Royal Society of Chemistry 2025

Org. Biomol. Chem., 2025, **23**, 2845–2853 | **2853**